Reprinted from Preprint Volume: Second Conference on Flash Floods. March 18-20, 1980, Atlanta, Ga. Published by the American Meteorological Society, Boston, Mass.

CAPABILITIES OF NWS MODEL TO FORECAST FLASH FLOODS CAUSED BY DAM FAILURES

D. L. Fread

Office of Hydrology, National Weather Service
Silver Spring, Maryland

1. INTRODUCTION

Catastrophic flooding occurs when a dam is breached and the impounded water escapes through the breach into the downstream valley. Usually the response time available for warning is much shorter than for precipitation-runoff floods. Dam failures are often caused by overtopping of the dam due to inadequate spillway capacity during large inflows to the reservoir from heavy precipitation runoff. In view of the short response time and the fact that dam-break floods are often coincident with heavy precipitation, this type of flood is indeed a flash flood.

The potential for catastrophic flooding due to dam failures has recently been brought to the Nation's attention by several dam failures such as the Buffalo Creek coal-waste dam, the Toccoa Dam, the Teton Dam, and the Laurel Run Dam. A report by the U.S. Army (1975) gives an inventory of the Nation's approximately 50,000 dams with heights greater than 25 ft. or storage volumes in excess of 50 acre-ft. The report also classifies some 20,000 of these as being "so located that failure of the dam could result in loss of human life and appreciable property damage...."

The National Weather Service (NWS) has the responsibility to advise the public of downstream flooding when there is a failure of a dam. Although this type of flood has many similarities to floods produced by precipitation runoff, the dam-break flood has some very important differences which make it difficult to analyze with the common techniques which have worked so well for the precipitation-runoff floods. To aid NWS flash flood hydrologists who are called upon to forecast the downstream flooding resulting from dam-failures, a numerical model (DAMBRK) has been recently developed. This paper presents an outline of the model's theoretical basis, its predictive capabilities, and some suggested ways of utilizing the model for real-time forecasting of dam-break floods.

2. MODEL DEVELOPMENT

The DAMBRK model represents the current state-of-the-art in understanding of dam failures and the utilization of hydrodynamic theory to predict the dam-break wave formation and downstream progression. The model has wide applicability; it can function with various levels of input data ranging from rough estimates to complete data specification; the required data is readily accessible; and it is economically feasible to use, i.e., it requires a minimal computation effort on large computing facilities.

The model consists of three functional parts, namely: (1) description of the dam failure mode, i.e., the temporal and geometrical description of the breach; (2) computation of the time history (hydrograph) of the outflow through the breach as affected by the breach description, reservoir inflow, reservoir storage characteristics, spillway outflows, and downstream tailwater elevations; and (3) routing of the outflow hydrograph through the downstream valley in order to determine the changes in the hydrograph due to valley storage, frictional resistance, downstream bridges or dams, and to determine the resulting water surface elevations (stages) and flood-wave travel times.

2.1 Breach Description

The breach is the opening formed in the dam as it fails. The actual failure mechanics are not well understood for either earthen or concrete dams. In previous attempts to predict downstream flooding due to dam failures, it was usually assumed that the dam failed completely and instantaneously. This assumption is somewhat appropriate for concrete arch-type dams but it is not appropriate for earthen dams and concrete gravity-type dams.

Earthen dams which exceedingly outnumber all other types of dams do not tend to completely fail nor do they fail instantaneously. The breach in earthen dams tends to have an average width ($\bar{b}$) in the range ($h_d < \bar{b} < 3h_d$) where h_d is the height of the dam. Breach widths for earthen dams are therefore usually much less than the total length of the dam as measured across the valley. Also, the breach requires a finite interval of time for its formation due to erosion of the dam materials by the escaping waters. Total time of failure may be in the range of a few minutes to a few hours, depending on the height of the dam, the type of materials used in construction, the extent of compaction of the materials, and the extent (magnitud and duration) of the overtopping flow of the escap ing waters. Piping failures occur when initial breach formation takes place at some point below the top of the dam due to erosion of an internal channel through the dam by escaping waters. As the erosion proceeds, a larger and larger opening is formed; this is eventually hastened by caving-in of the top portion of the dam.

Concrete gravity dams also tend to have a partial breach as one or more monolith sections formed during the construction of the dam are forced apart by the escaping waters. The time for breach formation is in the range of a few minutes.

Poorly constructed dams and coal-waste slag piles which impound waters tend to fail within a few minutes and have average breach widths in the upper range or even greater than those for the earthen dams mentioned above.

The NWS DAMBRK model allows the forecaster to input the failure time interval (τ) and the terminal size and shape of the breach (see Fig. 1). The shape is specified by a parameter (z) identifying the side slope of the breach, i.e., 1 vertical: z horizontal slope. The range of z values is: $0 \leq z \leq 2$. Rectangular, triangular, or trapezoidal shapes may be specified in this way. The final breach size is controlled by the z and another parameter (BB) which is the terminal width of the bottom of the breach. The model assumes the breach bottom width starts at a point and enlarges at a linear rate over the failure time interval (τ) until the terminal width is attained.

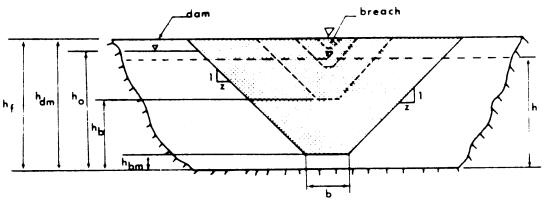

Figure 1. Front view of dam showing breach formation.

During the simulation of a dam failure, the actual breach formation commences when the water surface elevation (h) within the reservoir formed by the dam exceeds a specified value, h_f. This feature permits the simulation of an overtopping of a dam in which the breach does not form until a sufficient amount of water is flowing over the crest of the dam. A piping failure may be simulated when h_f is specified less than the height of the dam, h_d.

Selection of breach parameters before a breach forms, or in the absence of observations, introduces a varying degree of uncertainty in the forecast model; however, errors in the breach description and thence in the resulting time rate of volume outflow are rapidly damped-out as the flood wave advances downstream. For conservative forecasts which error on the side of larger flood waves, values for BB and z should produce an average breach width ($\bar{b}$) in the uppermost range for a certain type of dam. Failure time (τ) should be selected in the lower range to produce a maximum outflow. Of course, observational estimates of $\bar{b}$ and τ should be used when available to update forecasts when response time is sufficient as in the case of forecast points several miles downstream of the structure. Flood wave travel rates are often in the range of 2-10 miles per hour. Accordingly, response times for some downstream forecast points may therefore be sufficient for updated forecasts to be issued.

2.2 Reservoir Outflow Hydrograph

The total reservoir outflow consists of broad-crested weir flow through the breach and flow through any spillway outlets, i.e.,

$$Q = Q_b + Q_s \tag{1}$$

The breach outlfow (Q_b) is computed as:

$$Q_b = c_1(h-h_b)^{1.5} + c_2(h-h_b)^{2.5} \tag{2}$$

where:

$$c_1 = 3.1\, b_i\, c_v\, k_s \tag{3}$$

$$c_2 = 2.45\, z\, c_v\, k_s \tag{4}$$

$$b_i = BB\, t_b/\tau \tag{5}$$

$$c_v = 1.0 + 0.023\, Q^2/[B_d^2 h^2 (h-h_b)] \tag{6}$$

$$k_s = 1.0 \quad \text{if } \frac{h_t-h_b}{h-h_b} < 0.67 \tag{7}$$

otherwise:

$$k_s = 1.0 - 27.8\left(\frac{h_t-h_b}{h-h_b} - 0.67\right)^3 \tag{8}$$

in which h_b is the elevation of the breach bottom, h is the reservoir water surface elevation, b_i is the instantaneous breach bottom width, t_b is time after breach starts forming, c_v is correction for velocity of approach, Q is the total outflow from the reservoir, B_d is width of the reservoir at the dam, k_s is the submergence correction for tailwater effects on weir outflow, and h_t is the tailwater elevation (water surface elevation immediately downstream of dam).

The spillway outflow (Q_s) is computed as:

$$Q_s = c_s(h-h_s)^{1.5} + c_g(h-h_g)^{0.5} + c_d(h-h_d)^{1.5} + Q_t \tag{9}$$

in which c_s is the uncontrolled spillway discharge coefficient, h_s is the uncontrolled spillway crest elevation, c_g is the gated spillway discharge coefficient, h_g is the center-line elevation of the gated spillway, c_d is the discharge coefficient for flow over the crest of the dam, and Q_t is a constant outflow term which is head independent.

The total outflow is a function of the water surface elevation (h). Depletion of the reservoir storage volume by the outflow causes a decrease in h which then causes a decrease in Q. However, any inflow to the reservoir tends to increase h and Q. In order to determine the total outflow (Q) as function of time, the simultaneous effects of reservoir storage characteristics and reservoir inflow require the use of a reservoir routing technique. DAMBRK utilizes a hydrologic storage routing technique based on the law of conservation of mass, i.e.,

$$I - Q = dS/dt \tag{10}$$

in which I is the reservoir inflow, Q is the total reservoir outflow, and dS/dt is the time rate of change of reservoir storage volume. Eq. (9) may be expressed in finite difference form as:

$$(I+I')/2 - (Q+Q')/2 = \Delta S/\Delta t \tag{11}$$

in which the prime (') superscript denotes values at the time $t-\Delta t$ and the Δ approximates the differential. The term ΔS may be expressed as

$$\Delta S = (A_s+A_s')\,(h-h')/2 \tag{12}$$

in which A_s is the reservoir surface area coincident with the elevation (h).

Combining Eqs. (1), (2), (9), (11) and (12) result in the following expression:

$$(A_s+A_s')\,(h-h')/\Delta t + c_1(h-h_b)^{1.5} + c_2(h-h_b)^{2.5} + c_s(h-h_b)^{1.5} + c_g(h-h_g)^{0.5} + c_d(h-h_d)^{1.5} + Q_t + Q' - I - I' = 0 \tag{13}$$

Since A_s is a function of h and all other terms except h are known, Eq. (13) can be solved for the unknown h using Newton-Raphson iteration. Once h

is obtained, Eqs. (2) and (9) can be used to obtain the total outflow (Q) at time (t). In this way the outflow hydrograph Q(t) can be developed for each time (t) as t goes from zero to some terminating value (t_e) sufficiently large for the reservoir to be drained. In Eq. 13 the time step (Δt) is chosen sufficiently small to incur minimal numerical integration error. This value is preset in the model to $\tau/50$.

2.3 Downstream Routing

After computing the hydrograph of the reservoir outflow, the extent of and time of occurrence of flooding in the downstream valley is determined by routing the outflow hydrograph through the valley. The hydrograph is modified (attenuated, lagged, and distorted) as it is routed through the valley due to the effects of valley storage, frictional resistance to flow, and downstream obstructions and/or flow control structures. Modifications to the dam-break flood wave are manifested as attenuation of the flood peak elevation, spreading-out or dispersion of the flood wave volume, and changes in the celerity (translation speed) or travel time of the flood wave. If the downstream valley contains significant storage volume such as a wide flood plain, the flood wave can be extensively attenuated and its time of travel greatly increased. Even when the downstream valley approaches that of a uniform rectangular-shaped section, there is appreciable attenuation of flood peak and reduction in wave celerity as the wave progresses through the valley.

A distinguishing feature of dam-break waves is the great magnitude of peak discharge when compared to runoff-generated flood waves having occurred in the past in the same valley. The dam-break flood is usually many times greater than the runoff flood of record. The above-record discharges make it necessary to extrapolate certain coefficients used in various flood routing techniques and make it impossible to fully calibrate the routing technique.

Another distinguishing characteristic of dam-break floods is the very short duration time, and particularly the extremely short time from beginning of rise until the occurrence of the peak. The time to peak is in almost all instances synonymous with the breach formation time (τ) and therefore is in the range of a few minutes to a few hours. This feature, coupled with the great magnitude of the peak discharge, causes the dam-break flood wave to have acceleration components of a far greater significance than those associated with a runoff-generated flood wave.

A hydraulic routing technique (dynamic routing) based on the complete equations of unsteady flow is used to route the dam-break flood hydrograph through the downstream valley. This method is derived from the original equations developed by Barre De Saint-Venant (1871). In this method the important acceleration effects are properly considered. Also, the only coefficient that must be extrapolated beyond the range of past experience is the coefficient of flow resistance. It so happens that this is usually not a sensitive parameter in effecting the modifications of the flood wave due to its progression through the downstream valley. The dynamic routing technique properly considers the effect of downstream constructions and flow control structures such as bridge-road embankments or dams.

The unsteady flow equations consist of a conservation of mass equation, i.e.,

$$\frac{\partial Q}{\partial x} + \frac{\partial (A+A_o)}{\partial t} - q = 0 \qquad (14)$$

and a conservation of momentum equation, i.e.,

$$\frac{\partial Q}{\partial t} + \frac{\partial (Q^2/A)}{\partial x} + gA\left(\frac{\partial h}{\partial x} + S_f + S_e\right) = 0 \qquad (15)$$

where A is the active cross-sectional area of flow, A_o is the inactive (off-channel storage) cross-sectional area, x is the longitudinal distance along the channel (valley), t is the time, q is the lateral inflow or outflow per linear distance along the channel (inflow is positive and outflow is negative in sign), g is the acceleration due to gravity, S_f is the friction slope, and S_e is the expansion-contraction slope. The friction slope is evaluated from Manning's equation for uniform, steady flow, i.e.,

$$S_f = \frac{n^2 |Q| Q}{2.21\, A^2\, R^{4/3}} \qquad (16)$$

in which n is the Manning coefficient of frictional resistance and R is hydraulic radius defined as A/B where B is top width of active cross-sectional area. The term S_e is defined as follows:

$$S_e = \frac{k\, \Delta(Q^2/A^2)}{2g\, \Delta x} \qquad (17)$$

in which k is the expansion-contraction coefficient varying from 0.0 to 1.0, and $\Delta(Q/A)^2$ is the difference in the term $(Q/A)^2$ at two adjacent cross-sections separated by a distance Δx.

Eqs. (14)-(15) were modified by the author (Fread, 1976) to better account for the differences in flood wave properties for flow occurring simultaneously in the river channel and the overbank flood plain of the downstream valley. As modified, Eqs. (14)-(15) become:

$$\frac{\partial (K_c Q)}{\partial x_c} + \frac{\partial (K_\ell Q)}{\partial x_\ell} + \frac{\partial (K_r Q)}{\partial x_r} + \frac{\partial A}{\partial t} - q = 0 \qquad (18)$$

$$\frac{\partial Q}{\partial t} + \frac{\partial (K_c^2 Q^2/A_c)}{\partial x_c} + \frac{\partial (K_\ell^2 Q^2/A_\ell)}{\partial x_\ell} + \frac{\partial (K_r Q^2/A_r)}{\partial x_r} + gA_c\left(\frac{\partial h}{\partial x_c} + S_{fc} + S_e\right) + gA_\ell\left(\frac{\partial h}{\partial x_c} + S_{f\ell}\right) + gA_r\left(\frac{\partial h}{\partial x_r} + S_{fr}\right) = 0 \qquad (19)$$

in which the subscripts $_c$, $_\ell$, and $_r$ represent the channel, left flood plain, and right flood plain sections, respectively. The parameters (K_c, K_ℓ, K_r) serve to proportion the total flow (Q) into channel flow, left flood-plain flow, and right flood-plain flow, respectively. These are defined as follows:

$$K_c = \frac{1}{1+k_\ell+k_r} \qquad (20)$$

$$K_\ell = \frac{k_\ell}{1+k_\ell+k_r} \qquad (21)$$

$$K_r = \frac{k_r}{1+k_\ell+k_r} \qquad (22)$$

in which

$$k_\ell = \frac{Q_\ell}{Q_c} = \frac{n_c}{n_\ell}\frac{A_\ell}{A_c}\left(\frac{R_\ell}{R_c}\right)^{2/3}\left(\frac{\Delta x_c}{\Delta x_\ell}\right)^{1/2} \quad (23)$$

$$k_r = \frac{Q_r}{Q_c} = \frac{n_c}{n_r}\frac{A_r}{A_c}\left(\frac{R_r}{R_c}\right)^{2/3}\left(\frac{\Delta x_c}{\Delta x_r}\right)^{1/2} \quad (24)$$

Eqs. (23)-(24) represent the ratio of flow in the channel section to flow in the left and right flood-plain (overbank) sections, where the flows are expressed in terms of the Manning equation in which the energy slope is approximated by the water surface slope ($\Delta h/\Delta x$).

The friction slope terms in Eq. (19) are given by the following:

$$S_{fc} = \frac{n_c^2 |K_c Q| K_c Q}{2.21\, A_c^2\, R_c^{4/3}} \quad (25)$$

$$S_{f\ell} = \frac{n_\ell^2 |K_\ell Q| K_\ell Q}{2.21\, A_\ell^2\, R_\ell^{4/3}} \quad (26)$$

$$S_{fr} = \frac{n_r^2 |K_r Q| K_r Q}{2.21\, A_r^2\, R_r^{4/3}} \quad (27)$$

In Eq. (18), the term A is the total cross-sectional area, i.e.,

$$A = A_c + A_\ell + A_r + A_o \quad (28)$$

where A_o is the off-channel storage (inactive) area.

Either Eqs. (14)-(15) or Eqs. (18)-(19), which are non-linear partial differential equations, must be solved by numerical techniques. An implicit 4-pt. finite difference technique is used to obtain a solution to either set of equations. This particular technique (Fread, 1974) is used for its computational efficiency, flexibility, and convenience in the application of the equations to flow in complex channels existing in nature. In essence, the technique determines the unknown quantities (Q and h) at all specified cross-sections along the downstream channel-valley at various times into the future; the solution is advanced from one time to a future time by a finite time interval (time step) of magnitude Δt. The flow equations are expressed in finite difference form for all cross-sections along the valley and then solved simultaneously for the unknowns (Q and h) at each cross-section. Due to the non-linearity of the partial differential equations and their finite difference representations, the solution is iterative and a highly efficient quadratic iterative technique known as the Newton-Raphson method is used. Convergence of the iterative technique is attained when the difference between successive iterative solutions for each unknown is less than a relatively small prescribed tolerance. Usually, one to three iterations at each time step are sufficient for convergence to be attained for each unknown at all cross-sections. A more complete description of the solution technique may be found elsewhere (Amein and Fang, 1970; Fread, 1974; Fread, 1977).

The forecaster has the option to use either Eqs. (14)-(15) or Eqs. (18)-(19). The former is a somewhat simpler treatment in which a total or composite cross-section is used, whereas the latter set utilizes a more detailed representation of the flow cross-section. Eqs. (18)-(19) are recommended when the channel is sufficiently large to carry a significant portion of the total flow and the channel has a rather meandrous path through the downstream valley.

2.4 Initial and Boundary Conditions

In order to solve the unsteady flow equations the state of the flow (h and Q) must be known at all cross-sections at the beginning (t=o) of the simulation. This is known as the initial condition of the flow. The DAMBRK model assumes the flow to be steady, non-uniform flow where the flow at each cross-section is initially computed to be:

$$Q_i = Q_{i-1} + q_{i-1}\,\Delta x_{i-1} \qquad i=2,3,\ldots N \quad (29)$$

where Q_1 is the known steady discharge at the dam, i.e., the upstream boundary of the downstream valley, and q_i is any lateral inflow from tributaries existing between the cross-sections spaced at intervals of Δx along the valley. The steady discharge from the dam at t=o must be non-zero, i.e., a dry downstream channel is not amenable to simulation by DAMBRK. This is not an important restriction, especially when maximum flows and peak stages are of paramount interest in the dam-break flood. The tributary lateral inflow must be specified by the forecaster throughout the simulation period. If these flows are relatively small, they may be safely ignored.

The water surface elevations associated with the steady flow must also be computed at t=o. This is accomplished by solving the following equation:

$$\frac{(Q^2/A)_{i+1} - (Q^2/A)_i}{\Delta x_i} + g\left(\frac{A_i+A_{i+1}}{2}\right)\left(\frac{h_{i+1}-h_i}{\Delta x_i} + \frac{n^2(Q_i+Q_{i+1})^2(B_i+B_{i+1})^{4/3}}{2.2\,(A_i+A_{i+1})^{10/3}}\right) = 0 \quad (30)$$

This equation may be easily solved using the Newton-Raphson method by starting at a specified elevation at the downstream extremity of the valley and solving for the adjacent upstream elevation step by step until the upstream boundary is reached. The downstream specified elevation may be obtained from a solution of the Manning equation if the flow is governed only by the channel conditions; however, if a flow control structure produces a backing-up of the flow at this location, the forecaster must directly specify the water surface elevation existing at the downstream boundary at t=o.

In addition to initial conditions, boundary conditions at the upstream and downstream sections of the valley must be specified for all times (t=0 to t=t_e where t_e is the future time at which the simulation ceases).

At the upstream boundary the reservoir outflow hydrograph Q(t) provides the necessary boundary condition.

At the downstream boundary an appropriate stage-discharge relation is used. If the flow at the downstream extremity is channel-controlled, the following relation is used:

$$Q_N = \frac{1.49}{n} A_N^{5/3}/B_N^{2/3}\left(\frac{h_{N-1}-h_N}{\Delta x_{N-1}}\right)^{1/2} \quad (31)$$

Eq. (31) reproduces the hysteresis effect in stage-discharge relations often observed as a loop-rating curve. The loop (hysteresis) is produced by the temporal variations in the surface

slope. If the flow at the downstream boundary is controlled by a flow control structure such as a dam, the following relation is used:

$$Q_N = Q_b + Q_s \quad (32)$$

where the breach flow (Q_b) is defined by Eq.(2) and the spillway flow (Q_s) is defined by Eq. (9) in which the various terms apply to the dam at the downstream boundary. Since the resulting expressions for Q_b and Q_s are in terms of the water surface elevation h_N, Eq. (32) is a stage-discharge relation.

2.5 Multiple Dams and Bridges

The dam-break flood forecasting model can simulate the progression of a dam-break wave through a downstream valley containing a reservoir created by another downstream dam, which itself may fail due to being sufficiently overtopped by the wave produced by the failure of the upstream dam. In fact, an unlimited number of reservoirs located sequentially along the valley can be simulated. When the tailwater below a dam is affected by flow conditions downstream of the tailwater section (e.g., backwater produced by a downstream dam, flow constriction, bridge, and/or tributary inflow), the flow occurring at the dam is computed by using an internal boundary condition at the dam. In this method the dam is treated as a short Δx reach in which the flow through the reach is governed by the following two equations rather than either Eqs.(14)-(15) or Eqs. (18)-(19):

$$Q_i = Q_{i+1} \quad (33)$$

$$Q_i = Q_b + Q_s \quad (34)$$

in which Q_b and Q_s are breach flow and spillway flow as described in Eq. (32). In this way the flows Q_i and Q_{i+1} and the elevations h_i and h_{i+1} are in balance with the other flows and elevations occurring simultaneously throughout the entire flow system which may consist of additional dams which are treated as additional internal boundary conditions via Eqs. (33)-(34).

Highway/railway bridges and their associated earthen embankments which are located at points downstream of a dam may also be treated as internal boundary conditions. Eqs. (33)-(34) are used at each bridge; the term Q_s in Eq. (34) is computed by the following expression:

$$Q_s = C\sqrt{2g}\, A_{i+1}(h_i - h_{i+1})^{1/2} + C_d k_s (h - h_c)^{3/2} \quad (35)$$

in which C is a coefficient of bridge flow, C_d is the coefficient of flow over the crest of the road embankment, h_c is the crest elevation of the embankment, and k_s is similar to Eqs. (7)-(8).

2.6 Supercritical Flow

The DAMBRK model can simulate the flow through the downstream valley when the flow is supercritical. This type of flow occurs when the slope of the downstream valley exceeds about 50 ft/mi. Slopes less than this usually result in the flow being subcritical to which all preceding comments pertaining to the downstream routing apply. When the flow is supercritical, any flow disturbances cannot travel back upstream; therefore, the downstream boundary becomes superfluous. Thus, for supercritical flow, a downstream boundary condition is not required; however, an additional equation other than the reservoir outflow hydrograph is needed. To satisfy this requirement, an equation similar to Eq. (31) is used at the upstream boundary. Multiple reservoirs on supercritical valley slopes must be treated using a storage routing technique such as Eq. (13) rather than the dynamic routing technique.

2.7 Landslide Generated Waves

Reservoirs are sometimes subject to landslides which rush into the reservoir displacing a portion of the reservoir contents, and thereby creating a very steep water wave which travels up and down the length of the reservoir. This wave may have sufficient amplitude to overtop the dam and precipitate a failure of the dam, or the wave by itself may be large enough to cause catastrophic flooding downstream of the dam without resulting in the failure of the dam as perhaps in the case of a concrete dam.

The capability to generate waves produced by landslides is provided within DAMBRK. The volume of the landslide mass, its porosity, and time interval over which the landslide occurs, are input to the model. Within the model, the landslide mass is deposited within the reservoir in layers during small computational time steps, and simultaneously the original dimensions of the reservoir are reduced accordingly. The time rate of reduction in the reservoir cross-sectional area creates the wave during the solution of the unsteady flow Eqs. (14)-(15), which are applied to the cross-sections describing the reservoir characteristics.

3. DATA REQUIREMENTS

The DAMBRK model was developed so as to require data that was accessible to the forecaster. The input data requirements are flexible insofar as much of the data may be ignored (left blank on the input data cards or omitted altogether) when a detailed analysis of a dam-break flood inundation event is not feasible due to lack of data or insufficient data preparation time. Nonetheless, the resulting approximate analysis is more accurate and convenient to obtain than that which could be computed by other techniques. The input data can be categorized into two groups.

The first data group pertains to the dam (the breach, spillways, and reservoir storage volume). The breach data consists of the following parameters: τ (failure time of breach, in hours); BB (final bottom width of breach); z (side slope of breach); h_{bm} (final elevation of breach bottom); h_o (initial elevation of water in reservoir); h_f (elevation of water when breach begins to form); and h_d (elevation of top of dam). The spillway data consists of the following: h_s (elevation of uncontrolled spillway crest); c_s (coefficient of discharge of uncontrolled spillway); h_g (elevation of center of submerged gated spillway); c_g (coefficient of discharge of gated spillway); c_d (coefficient of discharge of crest of dam); and Q_t (constant, head independent discharge from dam). The storage parameters consist of the following: a table of surface area (A_s) in acres or volume in acre-ft. and the corresponding elevations within the reservoir. The forecaster must estimate the values of τ, BB, z, h_{bm}, and h_f. The remaining values are obtained from the physical description of the dam, spillways, and reservoir. In some cases, h_s, c_s, h_g, c_g, and c_d may be ignored and Q_t used in their place.

The second group pertains to the routing of the outflow hydrograph through the downstream

valley. This consists of a description of the cross-sections, hydraulic resistance coefficients, and expansion coefficients. The cross-sections are specified by location mileage, and tables of top width (active and inactive) and corresponding elevations. The active top widths may be total widths as for a composite section, or they may be left flood plain, right flood plain, and channel widths. The top widths can be obtained from USGS topography maps, 7 1/2' series, scale 1:24000. The channel widths are usually not as significant for an accurate analysis as the overbank widths (the latter are available from the topo maps). The number of cross-sections used to describe the downstream valley depends on the variability of the valley widths. A minimum of two must be used. Additional cross-sections are created by the model via linear interpolation between adjacent cross-sections specified by the forecaster. This feature enables only a minimum of cross-sectional data to be input by the forecaster according to such criteria as data availability, variation, preparation time, etc. The number of interpolated cross-sections created by the model is controlled by the parameter DXM which is input for each reach between specified cross-sections. The hydraulic resistance coefficients consist of a table of Manning's n vs. elevation for each reach between specified cross-sections. The expansion-contraction coefficients (k) are specified as non-zero values at sections where significant expansion or contractions occur. The DXM and k parameters may be left blank in most analyses.

4. MODEL TESTING

The DAMBRK model has been tested on five historical dam-break floods to determine its ability to reconstitute observed downstream peak stages, discharges, and travel times. Those floods that have been used in the testing are: 1976 Teton Dam, 1972 Buffalo Creek Coal-Waste Dam, 1889 Johnstown Dam, 1977 Toccoa (Kelly Barnes) Dam, and the 1977 Laurel Run Dam floods. However, only the Teton flood will be presented herein.

The Teton Dam, a 300 ft. high earthen dam with a 3,000 ft. long crest, failed on June 5, 1976, killing 11 people, making 25,000 homeless, and inflicting about $400 million in damages to the downstream Teton-Snake River Valley. Data from a Geological Survey Report by Ray, et al. (1977) provided observations on the approximate development of the breach, description of the reservoir storage, downstream cross-sections and estimates of Manning's n approximately every 5 miles, indirect peak discharge measurements at 3 sites, flood peak travel times, and flood peak elevations. The inundated area is shown in Fig. 2.

The following breach parameters were used in DAMBRK to reconstitute the downstream flooding due to the failure of Teton Dam: τ = 1.25 hrs., BB = 150 ft., z = 0, h_{bm} = 0.0, h_f = h_d = h_o = 261.5 ft. Cross-sectional properties at 12 locations shown in Fig. 2 along the 60-mile reach of the Teton-Snake River Valley below the dam were used. Five top widths were used to describe each cross-section. The downstream valley consisted of a narrow canyon (approx. 1,000 ft. wide) for the first 5 miles and thereafter a wide valley which was inundated to a width of about 9 miles. Manning's n values ranging from 0.028 to 0.047 were provided from field estimates by the Geological Survey. DXM values between cross-sections

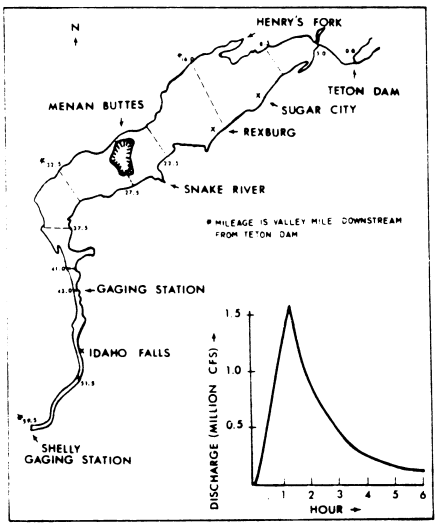

Figure 2. Flooded area downstream of Teton Dam and computed outflow hydrograph at dam.

were assigned values that gradually increased from 0.5 miles near the dam, to a value of 1.5 miles near the downstream boundary at the Shelly gaging station (valley mile 59.5 downstream from the dam). The reservoir surface area-elevation values were obtained from Geological Survey topo maps. The downstream boundary was assumed to be channel flow control as represented by a loop rating curve given by Eq. (31).

The computed outflow hydrograph is shown in Fig. 2. It has a peak value of 1,652,300 cfs (cubic feet per second), a time to peak of 1.25 hrs., and a total duration of about 6 hrs. The peak is about 20 times greater than the flood of record. The temporal variation of the computed outflow volume compared within 5 percent of observed values. The computed peak discharge values along the 60-mile downstream valley are shown in Fig. 3 along with three observed (indirect measurement) values at miles 8.5, 43.0, and 59.5. The average difference between the computed and observed values is 4.8 percent. Most apparent is

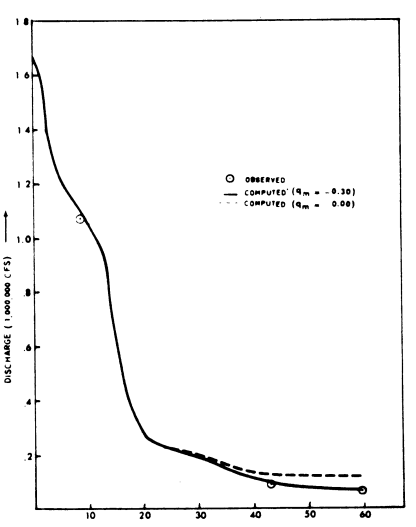

Figure 3. Profile of peak discharge from Teton Dam failure.

the extreme attenuation of the peak discharge as the flood wave progresses through the valley. Two computed curves are shown in Fig. 3; one in which no losses were assumed, i.e., $q_m = 0$; and a second in which the losses were assumed to be uniform along the valley. The losses were assumed to vary from 0 to a maximum of $q_m = -0.30$ and were accounted for in the model through the q term in Eq. (14). Losses were due to infiltration and detention storage behind irrigation levees.

The a priori selection of the breach parameters (τ and BB) causes the greatest uncertainty in forecasting dam-break flood waves. The sensitivity of downstream peak discharges to reasonable variations in τ and $\bar{b}$ is shown in Fig. 4.

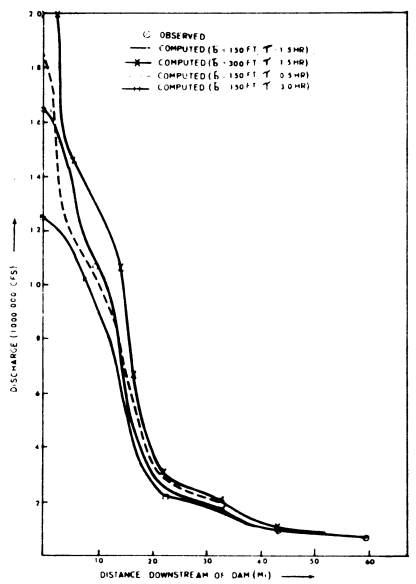

Figure 4. Profile of peak discharges from Teton Dam failure showing sensitivity to τ and $\bar{b}$ parameters.

Although there are large differences in the discharges (+45 to -25 percent) near the dam, these rapidly diminish in the downstream direction. After 10 miles the variation is +20 to -14 percent, and after 15 miles the variation has further diminished (+15 to -8 percent). The tendency for extreme peak attenuation and rapid damping of differences in the peak discharge is accentuated in the case of Teton Dam due to the presence of the very wide valley. Had the narrow canyon extended all along the 60-mile reach to Shelly, the peak discharge would not have attenuated as much and the differences in peak discharges due to variations in τ and $\bar{b}$ would be more persistent. In this instance, the peak discharge would have attenuated to about 350,000 rather than 67,000 as shown in Fig. 4, and the differences in peak discharges at mile 59.5 would have been about 27 percent as opposed to less than 5 percent as shown in Fig. 4.

Computed peak elevations compared favorably with observed values. The average absolute error was 1.5 ft., while the average arithmetic error was only -0.2 ft.

The computed flood peak travel times and three observed values are shown in Fig. 5. The differences between the computed and observed are about 10 percent for the case of using the estimated Manning's n values and about 1 percent if

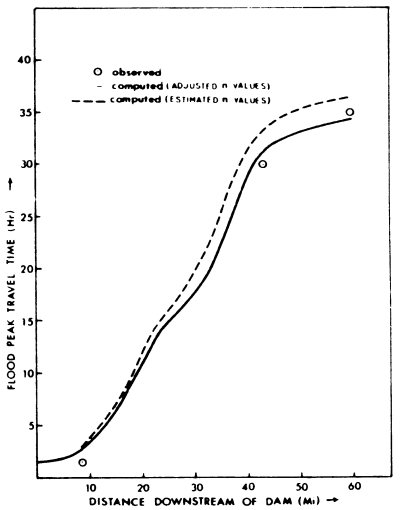

Figure 5. Flood peak time of travel to points downstream of Teton Dam.

the n values are slightly increased by 7 percent.

As mentioned previously, the Manning's n must be estimated, especially for the flows above the flood of record. The sensitivity of the computed stages and discharges of the Teton flood due to a substantial change (20 percent) in the Manning's n was found to be as follows: 1) 0.5 ft. in computed peak water surfce elevations or about 2 percent of the maximum flow depths, 2) 16 percent deviation in the computed peak discharges, 3) 0.8 percent change in the total attenuation of peak discharge incurred in the 60-mile reach from Teton Dam to Shelly, and 4) 15 percent change in the flood peak travel time to Shelly. These results indicate that Manning's n has little effect on peak elevations or depths; however, the travel time is affected by nearly the same percent that the n values are changed.

A typical simulation of the Teton flood as described above involved 78 Δx reaches, 55 hrs. of prototype time, and an initial time step (Δt) of 0.06 hrs. Such a simulation run required only 19 seconds of CPU time on an IBM 360/195 computer system; the associated cost was less than $5 per run.

Information on similar testing of DAMBRK on the Buffalo Creek flood can be found in Fread (1977). The results showed a similar degree of comparison between computed and observed values.

5. FORECAST APPLICATIONS

The NWS DAMBRK model is suitable for the following two types of forecasting applications: 1) pre-computation of flood peak elevations and travel times prior to a dam failure, and 2) real-time computation of the downstream flooding when a dam failure is imminent or has immediately occurred.

Pre-computations of dam failures enable the preparation of concise graphs or flash flood tables for use by those responsible for community preparedness downstream of critically located dams. The graphs provide information on flood peak elevations and travel times throughout the critical reach of the downstream valley. The variations in the pre-computed values due to uncertainty in the breach parameters (τ and $\bar{b}$) can be included in the graph. Results obtained using a maximum

probable estimate of $\bar{b}$ and a minimum probable estimate of τ would define the upper envelope of probable flood peak elevations and minimum travel times. Similarly, the use of a minimum probable estimated $\bar{b}$, along with a maximum probable estimate of τ, would define the lower limit of the envelope of probable peak elevations and maximum travel times. In the pre-computation mode, the forecaster can use as much of the capabilities of the DAMBRK model as time and data availability warrant.

Real-time computation is also possible in certain situations where the total response time for a dam-break flood warning exceeds a few hours. An abbreviated data input to DAMBRK can be used to quickly compute an approximate crest profile and arrival times. Computer coding forms have been prepared by the NWS Ft. Worth River Forecast Center with invariable parameters delineated and essential input data flagged. Using available topo maps and a minimum of information on the dam such as its height and storage volume, a forecast can be made within approximately 30 minutes.

In some cases it may be possible to make a revised forecast in real-time to update a pre-computed forecast when observations of the extent of the breach are made available to the forecaster. This would be valuable in refining the forecast for communities located far downstream where the possibility of flood inundation is questionable and the need for eventual evacuation can be more accurately defined by utilizing observations at the dam or actual flood elevations observed a few miles below the dam. The data set used to make the real-time update of the pre-computed forecast would have been retrieved from a data storage system and the critical parameters therein changed.

6. SUMMARY AND CONCLUSIONS

A dam-break flood forecasting model (DAMBRK) is described and applied to an actual dam-break flood wave. The model consists of a breach component which utilizes simple parameters to provide a temporal and geometrical description of the breach. A second component computes the reservoir outflow hydrograph resulting from the breach via a broad-crested weir-flow approximation, which includes effects of submergence from downstream tailwater depths and corrections for approach velocities. Also, the effects of storage depletion and upstream inflows on the computed outflow hydrograph are accounted for through storage routing within the reservoir. The third component consists of a dynamic routing technique for determining the modifications to the dam-break flood wave as it advances through the downstream valley, including its travel time and resulting water surface elevations. The dynamic routing component is based on a weighted, four-point non-linear finite difference solution of the one-dimensional equations of unsteady flow. Provisions are included for routing supercritical flows as well as subcritical flows, and incorporating the effects of downstream obstructions such as road-bridge embankments and/or other dams.

Model data requirements are flexible, allowing minimal data input when it is not available while permitting extensive data to be used when appropriate.

The model was tested on the Teton Dam failure. Computed outflow volume through the breach coincided with the observed values in magnitude and timing. Observed peak discharges along the downstream valley were satisfactorily reproduced by the model even though the flood wave was severely attenuated as it advanced downstream. The computed peak flood elevations were within an average of 1.5 ft. of the observed maximum elevations. The Teton application indicated an important lack of sensitivity of downstream discharge to errors in the forecast of the breach size and timing. Such errors produced significant differences in the peak discharge in the vicinity of the dam; however, the differences were rapidly reduced as the wave advanced downstream. Computational requirements of the model are quite feasible; CPU time (IBM 360/195) was 0.008 second per hr. per mile of prototype dimensions for the Teton Dam application.

Suggested ways for using the DAMBRK model in preparation of pre-computed flood information and in real-time forecasting were presented.

REFERENCES

Amein, M., and C. S. Fang, 1970: Implicit flood routing in natural channels. J. Hydraulic Div., ASCE, 96, HY12, Dec., 2481-2500.

De Saint-Venant, Barre, 1871: Theory of unsteady water flow, with application to river floods nels. Acad. Sci. (Paris) Comptes rendus, 73, 237-240.

Fread, D. L., 1974: Numerical properties of implicit four-point finite difference equations of unsteady flow. NOAA Tech Memo, NWS HYDRO-18, U.S. Dept. of Commerce, NOAA, National Weather Service, 38 pp.

Fread, D. L., 1976: Flood routing in meandering rivers with flood plains, Proceedings, Rivers '76, Third Ann. Symp. of Waterways, Harbors and Coastal Eng. Div., ASCE, Vol. I, Aug., 16-35.

Fread, D. L., 1977: The development and testing of a dam-break flood forecasting model, Proc., Dam-Break Flood Modeling Workshop, U.S. Water Res. Council, Wash., D.C., 1977, 164-197.

Ray, H. A., L. C. Kjelstrom, E. G. Crosthwaite, and W. H. Low, 1976: The flood in southeastern Idaho from the Teton Dam failure of June 5, 1976. Unpublished open file report, U.S. Geological Survey, Boise, Idaho.

U.S. Army Corps of Engineers, 1975: National Program of Inspection of Dams, Vol. I-V, Dept. of the Army, Office of Chief of Engineers, Wash., D.C.